◆ Human Brain Mapping 10:49–60(2000) ◆

ERPs and PET Analysis of Time Perception: Spatial and Temporal Brain Mapping During Visual Discrimination Tasks

Viviane Pouthas,* Line Garnero, Anne-Marie Ferrandez, and Bernard Renault

Unité de Neurosciences Cognitives et Imagerie Cérébrale, Hôpital de la Salpêtrière, Paris, France

Abstract: ERPs were recorded from 12 subjects performing duration and intensity visual discrimination tasks which have been previously used in a PET study. PET data showed that the same network was activated in both tasks [P. Maquet et al., NeuroImage 3:119–126, 1996]. Different ERP waveforms were observed for the late latency components depending on the dimension of the stimulus to be processed: frontal negativity (CNV) for the duration task and parieto-occipital positivity (P300) for the intensity task. Using BESA software, the sources were first modelled with a "PET dipolar model" (right prefrontal, right parietal, anterior cingulate, left and right fusiforms). To obtain a better fit for ERPs recorded in each task, two sources (cuneus, left prefrontal area) had to be added. Consistently with PET findings, dipole modelling indicates that duration and intensity dimensions of a visual stimulus are processed in the same areas. However, ERPs also reveal prominent differences between the time course of the dipole activations for each task, particularly for sources contributing to the late latency ERP components. In the intensity task, dipoles located in the cuneus, the anterior cingulate, and the left prefrontal area yield largest activity within the P300 interval, then activity diminishes rapidly as the stimulus ends, whereas in the duration task, the cuneus and anterior cingulate are still active several hundred milliseconds following stimulus offset. Moreover, in the duration task, the activity of the right frontal dipole parallels the CNV waveform, whereas in the intensity task, this dipole is largely inactive. We assume that the right frontal area plays a specific role in the formation of temporal judgments. *Hum. Brain Mapping 10:49–60, 2000.*

Key words: visual discrimination; time; intensity; event-related potentials; PET; prefrontal cortex; extrastriate areas

INTRODUCTION

Time is clearly a source of information which shapes one's behavior. Indeed in our everyday life, we are often confronted to a wide range of durations to which we frequently adapt. For example, we have to discriminate the duration of linguistic sounds and accurately pause between sentences and speaking turns, to achieve optimal communication; when we drive, we know the duration of the traffic lights in our familiar neighbourhood and anticipate the right moment to start again. Thus, as stressed by Elbert et al. [1991] "the preparation of efficient behavior, for example for a fast response, certainly benefits from predicting precisely the point in time." In spite of its importance, however, nobody has yet evidenced any sense or sense organ by

*Correspondence to: Viviane Pouthas, Unité de Neurosciences Cognitives et Imagerie Cérébrale, UPR 640 CNRS, LENA, Hôpital de la Salpêtrière, 47 Boulevard de l'Hôpital, 75651 Paris Cedex, France. E-mail: lenavp@ext.jussieu.fr

Received 1 November 1999; accepted 3 March 2000

which time can be directly perceived. Furthermore, the question of how duration is estimated by our information processing system remains a matter of debate. Some authors state that time is not a perceptual dimension [Gibson, 1975] but a "derived entity" in the conscious experience [Michon, 1990]. It is only recently that studies using functional brain mapping explored the possible locations where time-related attributes of stimuli or actions are processed [Coull and Nobre, 1998; Hinton et al., 1996; Jueptner et al., 1995; Lejeune et al., 1997; Maquet et al., 1996], whereas the cerebral structures involved in the perception of environmental dimensions, such as intensity, pitch, color, and shape or spatial location of auditory and visual stimuli, start to be well-documented [see Cabeza and Nyberg, 1997 for a review].

The psychophysical models elaborated since the beginnings of experimental psychology have found a renewal of interest with the development of cognitive psychology. They provide a conceptual framework and analytic tools to guide the search for the neurobiological mechanisms of the interval timing capacity. The basic features of these models are common (i.e., the starting point is "the clock"), and two other important components are the memory and decision devices which translate clock readings into behavior [e.g., Church, 1984; Church and Broadbent, 1990; Michon, 1967; Treisman and Brogan, 1992]. Recently published neuropsychological as well as imagery data suggest that three main brain regions would be involved in the temporal information processing: the cerebellum, the basal ganglia, and the frontal cortex. Neuropsychological studies of cerebellar patients exhibit a poor discrimination of durations less than 1 sec and a great variability of rhythmic tapping as well as distortions in time estimation [Casini and Ivry, 1999; Ivry et al., 1988; Ivry and Keele, 1989]. This is also the case for patients with Parkinson's disease [Malapani et al., 1998]. Duration perception deficits are also associated with damage in the middle and superior right frontal gyri [Harrington et al., 1998]. Imaging studies show the activation of cerebellar areas [Jueptner et al., 1995; Maquet et al., 1996] and of the basal ganglia as well as the activation of the prefrontal cortex in tasks that require estimation of brief durations [Hinton et al., 1996] or timing of movements [Rao et al., 1997]. The implication of the prefrontal cortex has also been assessed using electrophysiological methods [Bruder et al., 1992; Casini and Macar, 1996; Elbert et al., 1991]. However, whatever the brain regions considered, it is difficult to specify their function regarding the temporal information processing per se, because one can argue that basal ganglia and cerebellum play an important role in motor control and that frontal areas are involved in attentional and mnesic processes.

Thus, much remains to be understood about the functional neuroanatomy of temporal information processing. For example, to conclude that the perception of a stimulus duration is, in itself, responsible for the pattern of activation observed, it should be demonstrated that this pattern is not elicited by the perception of another parameter of the stimulation. Therefore, in a previous PET study, we contrasted two visual discrimination tasks, one based on the duration of a visual stimulus and the other on the luminance of the same stimulus [Maquet et al., 1996]. Results showed that the same network was activated in both tasks—right prefrontal cortex, right inferior parietal lobule, anterior cingulate cortex, left fusiform gyrus, and vermis. Because both discrimination tasks involve similar attention level and memory load, we proposed that the recruitment of visual attention and memory structures could best explain the cortical maps obtained. Indeed, the activated cerebral areas share some similarities with the patterns of activation described in visuo-spatial working memory [Jonides et al., 1993] and visual attention [Pardo et al., 1991] tasks.

In our PET study, the stimulus durations were relatively short compared to interstimulus intervals (between 1500 and 2300 ms), which in fact lasted about 75% of the scanning time. As the PET method integrates tracer activity over a period of many seconds, its temporal resolution is insufficient to specify areas only involved when the subjects are processing the duration or intensity. Event-related potentials (ERPs), on the other hand, reflect the rapidly changing electrical activity in the brain evoked by a stimulus or a cognitive event, and thus allow one to discriminate between different stages in cognitive processing. It is difficult, however, to determine the neural sources of ERPs components. Therefore, we recorded ERPs from subjects performing duration and intensity tasks identical to those used in our PET study, and we combined both sets of data to test whether the spatio-temporal organization of the different activations could differentiate the underlying coding mechanisms involved in both tasks. PET and ERP data have been combined in recent studies [Heinze et al., 1994; Mangun et al., 1997; Woldorff et al., 1997] in which the analysis was restrained to the early and middle latency components only (N1 or P1) between 80 and 150 ms following stimulus onset, to study the early visual spatial attention; the modelization was thus focused on one or two generators only. Because the pattern of activation described in our PET study involved an extended network of brain structures, we assumed that these acti-

vations would probably correspond to neural activities associated with different and specific cognitive aspects of the tasks. The present study thus attempts to widen the modelling up to 1500 ms following the beginning of the trial to include the major contributing sources of slow waves (CNV and late P300) and of motor preparation components. In summary, the aim of the present study was to specify *when* the estimated sources were active and then to determine for which processing stages different cerebral areas were involved.

METHODS

Subjects and tasks

Subjects were 12 young (between 20 and 26 years of age) right-handed males with normal or corrected to normal vision. They performed the same two target tasks as in the PET study. In the duration task, the subjects had to evaluate whether the duration of illumination of a green LED (490, 595, 700, 805, and 910 ms) was equal to (right button press) or different from (left button press) that of a previously presented standard duration (700 ms). The intensity of each signal was 15 cd/m^2. The standard was presented six successive times before the beginning of the task, then each test stimulus for each duration including the standard one was presented 20 times in a random order, making a total of 100 trials. In the intensity task, the subjects had to judge whether the intensity of the LED (3, 7, 15, 22, and 29 cd/m^2) was equal to (right button press) or different from (left button press) that of a previously standard intensity (15 cd/m^2). Each signal lasted 700 ms. As in the duration task, the standard was presented six successive times before the beginning of the task, then each test stimulus for each intensity level including the standard one was presented 20 times in a random order, making a total of 100 trials. In each task, the ISI lasted between 1500 ms to 2300 ms (on average, 1900 ms). The subjects had to perform each task twice. The order was counterbalanced over subjects.

ERP data acquisition

Event-related potentials were simultaneously recorded from 31 electrodes at standard EEG sites with respect to ear-linked reference (sample rate per channel = 250 Hz, bandpass 0.16–80 Hz). Eye movements and blinks (EOG) were recorded by two bipolar electrodes for later rejection using an automatic eye-movement correction program [Gratton et al., 1983]. The length of the averaging window was 1500 ms with a 100 ms baseline interval prior to the LED switch on. ERP averages were computed from the pooled data of subjects for each task (duration and intensity). In the first stage of the analysis, all trials were averaged for the two target tasks whether the response was correct or not and whatever the duration of the LED illumination or whatever the intensity level. However, to proceed to a finer comparison of the ERP waveforms, we only averaged ERPs corresponding to the trials where the stimulus was similar in both tasks, that is, the standard stimulus (700 ms and 15 cd/m^2). On the other hand, Ruchkin et al.'s [1977] results suggest that the time course of the CNV wave correlates with temporal judgments. Therefore, for the duration task, to analyse in more detail the possible differences in the CNV related to the LED illumination duration, we averaged data of trials corresponding to each of the five durations (490, 595, 700, 805, and 910 ms).

Source analysis

The localization of the dipoles generating the electrical activity were then modelled using the BESA software [Scherg, 1992]. Because this modelling technique involves a large number of free parameters (three location, two orientation, and one magnitude parameters for each dipole) and because the EEG solutions are not unique, we first applied a "PET seeded model" transforming the Talairach coordinates corresponding to the activations observed in the PET study into BESA coordinates using a software developed by us. The proportional Talairach space is transformed into the BESA spherical model. The center of the sphere is placed at the posterior commissure (CP), and the range of the anterior Talairach coronal coordinates (anterior to CP) are fitted to the radius of the sphere, as well as the posterior part (posterior to CP). Similarly, the sagittal and axial coordinates are also transformed according to the BESA sphere radius using linear transformations. At the reverse, to transform BESA coordinates to Talairach space, the coordinates are rescaled so that the anterior part of the sphere matches with the Talairach anterior boxes (anterior to CP) and the posterior part of the sphere matches with the posterior to CP box. Our aim being to combine PET and EEG data, the "PET seeded model" was applied to ERP data corresponding to all trials of each target task. Then, examining the resulting differences between the ERP maps and the dipole maps we attempted to obtain a better fit solution by adding dipolar sources to the "PET model".

Furthermore, ERPs provide a tool to define the time course of different processing steps. Accordingly, in

the present study, we had the opportunity to check for possible differences in the time course of dipolar source activations between both tasks. To make the comparison meaningful, we applied the dipole model corresponding to the best-fit solution to data recorded for both tasks under trials where the timing was similar [i.e., under trials in which the standard stimulus was presented (700 ms duration)]. In this case, the only difference was the requirements of the task, either duration discrimination or intensity discrimination. Finally, in the duration task, we sought to determine whether the time course of the activity of the dipoles would depend on the duration of the LED illumination. Therefore, we applied the model to the EEG data recorded for the five different sets of trials corresponding to the five durations tested during the task.

RESULTS

Behavioral data

Figure 1 presents the average generalization gradients for the duration and the intensity tasks in both studies. This figure shows that the performances obtained during the ERP study are very similar to the previous results of the PET experiment.

ERP data

ERP waveforms averaged across subjects from the 31 electrodes for the duration and the intensity discrimination tasks are superimposed in Figure 2. Scrutiny of these waveforms suggests that there was no difference between the early and middle latency components observed during the duration and the intensity discrimination tasks. A positive wave developped between approximately 90 ms and 130 ms over parieto-occipital areas. Anovas revealed no effect of the discrimination type neither on the mean amplitude (POZ: +3.22 μv and +3.14 μv in the duration and in the intensity tasks, respectively [$F(1,11) = .54$, $p > .10$], nor on the mean latency [128 ms and 124 ms in the duration and in the intensity tasks, respectively, $F(1,11) = 1.57$, $p > .10$]. A negative component, maximal on P5 and P6 parietal electrodes, peaked around 180 ms. Anovas carried out on this component confirmed that there was no effect of the task, neither on its mean amplitude [P5: −2.15 μv, P6: −2.39 μv and P5: −2.06 μv, P6: −2.30 μv in the duration and in the intensity tasks, respectively, $F(1,11) = .44$, $p > .10$] nor on its mean latency [176 ms and 172 ms in the duration and in the intensity tasks, respectively, $F(1–11) = 0.02$, $p > .10$].

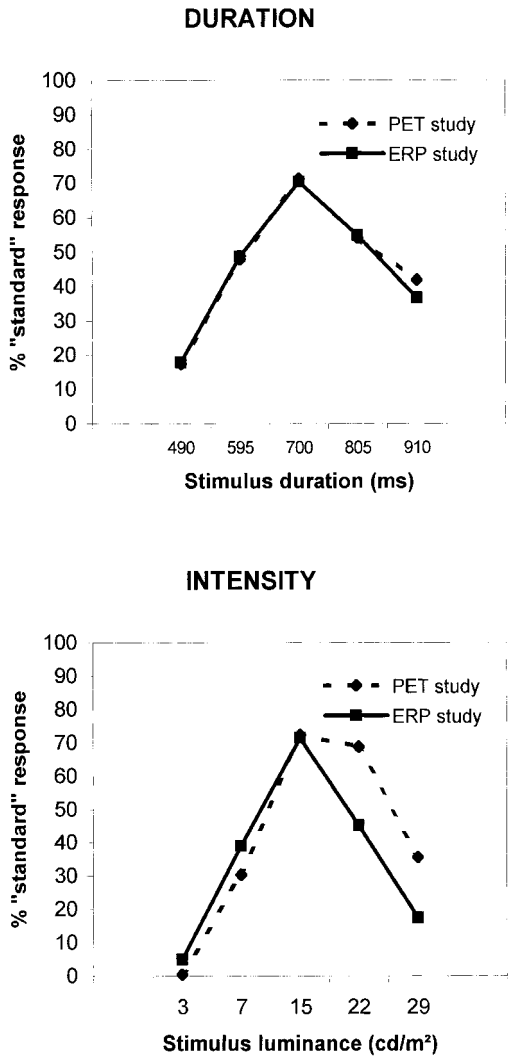

Figure 1.
Average generalization gradients: percentage of "equal to standard" responses (ordinate), stimulus value (abscissa).

As it is apparent from Figure 2, prominent differences emerged between both tasks for the late latency ERP components. The intensity task elicited a posteriorly distributed large positive wave that peaked around 500 ms following stimulus onset and a negativity of small amplitude over fronto-cental sites. The parieto-occipital positive component (late P3b) would probably reflect the end of the stimulus evaluation and the decision process. In contrast, the duration task elicited a large negative wave (CNV) distributed over fronto-central areas that peaked around 600 ms following stimulus onset. In this task also, the parieto-occipital positive component of the visual event-re-

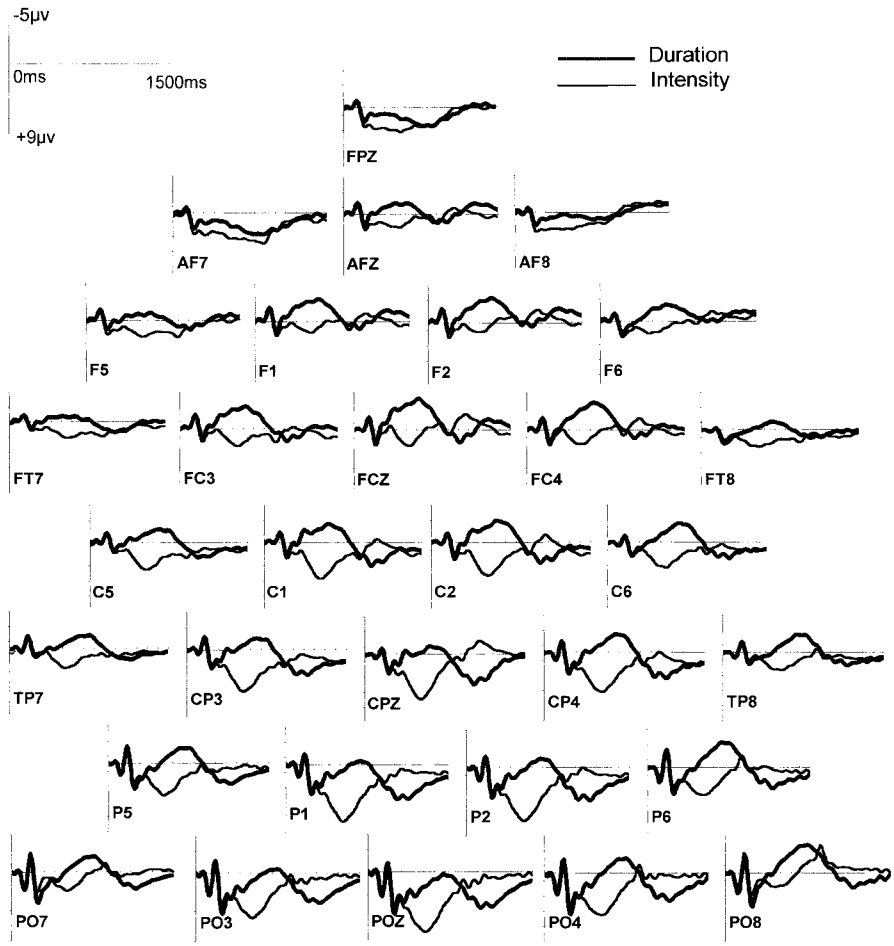

Figure 2.
ERP waveforms averaged across subjects from the 31 electrode sites, contrasting ERPs recorded for the duration and for the intensity tasks.

lated potential (P2) was followed by a negative shift. Then, a further late positive component was observed between 900 and 1300 ms on these posterior sites.

Many previous studies [Elbert et al., 1991; Macar and Vitton, 1980; Ruchkin et al., 1977; Walter et al., 1964; among others] revealed that the CNV followed by a positive shift would underlie the timing of the cognitive activity associated with the formation of the temporal judgment. To examine our data in more detail, we contrasted ERP waveforms recorded on FCZ for each of the five sets of trials corresponding to the five durations: they are superimposed in Figure 3. These waveforms indicate that there was a covariation between the duration of the LED illumination and the latency of ERPs zero crossing on FCZ. Differences in the latency of the zero crossing would reflect differences in the timing of the cognitive processes associated with subjects' temporal judgments and response selection.

In sum, the early and middle latency waves, that may be modulated by selective attention, were not affected by the dimension of the stimulus—intensity or duration—to be processed. In contrast, different ERP waveforms and topographies were observed for the late latency components, depending on which dimension of the stimulus the comparison with the standard held in memory had to be done: frontal negativity in the duration task and parieto-occipital positivity in the intensity task.

Dipole analysis

The strategy used to carry out the fusion of PET and ERP data was to derive a generator model accounting for the ERPs recorded during a large time window (100–1500 ms), corresponding to the time window during which subjects do perform the tasks. This would consequently implicate a large number of dipoles. The generators of the electrical activity were thus first modelled with a "PET seeded model". The Talairach coordinates corresponding to the activations observed in the PET study—right prefrontal cortex, right inferior parietal lobule, anterior cingulate cortex, left and right fusiform gyri—were transformed into

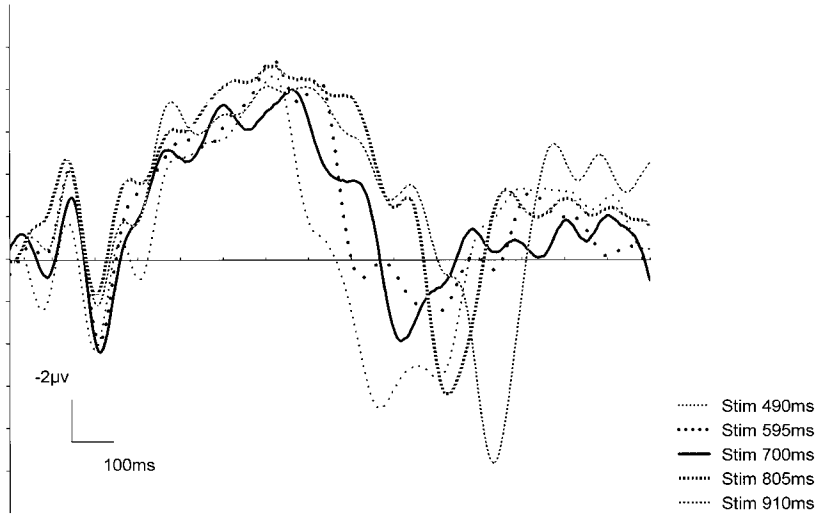

Figure 3.
CNVs: ERP waveforms recorded on the FCZ electrode for the five stimulus durations.

BESA coordinates. It should be noted that no significant activation was observed in the right fusiform gyrus during the duration task. However, the same "PET seeded model" was applied to ERP data recorded during both discrimination tasks, because no significant variation of rCBF was observed between them when they were contrasted. Furthermore, in our PET study, there was also a significant increase of the rCBF in the vermis, the electrical activity of which cannot be modelled. Each of the five dipolar sources was fixed in location but allowed to vary in orientation to fit the observed potential distributions. This "PET seeded model" accounted for 84.9% of the variance in the duration task and for 80.9% in the intensity one, over the 100–1500 ms time range. The difference maps (difference between the observed potential distribution and the scalp distribution that would be produced by the dipoles) obtained with the "PET seeded model" showed that the model poorly accounted for the ERPs recorded on two scalp areas (i.e., a left frontal area and a median occipital area), particularly between 400 and 800 ms following stimulus onset. This suggested that a better fit could be obtained with two additional dipoles.

Therefore, two dipolar sources were added; the first dipole was placed arbitrarily in a median occipital location and then allowed to vary from this starting value in both location and orientation to obtain the smallest residual variance between the model and the recorded ERP data. The transformation of BESA coordinates into Talairach coordinates revealed that this dipolar source was located in the cuneus. Then, a left frontal dipolar source was placed at a fixed location symmetrically to the right prefrontal one (area 45), but was allowed to vary in orientation and finally, all seven dipoles were allowed to vary in orientation and the best-fit solution over the 100–1500 ms time range was obtained. Figure 4 shows the position, orientation, and source waveform (magnitude over time) for each of the dipoles of the resulting seven dipole configuration which accounted for 94.9% of the variance in the data set of the duration task and for 90.5 % of the variance in the dataset of the intensity task over the 100–1500 ms time range. Figure 5 shows the locations of the seven dipoles in the Talairach coordinates.

This seven dipole solution accounting for all data (five levels of intensity or duration) was then applied only to the standard level ERP data recorded in both discrimination tasks. It also was applied to the ERPs obtained from the five duration levels. The resulting seven source waveforms obtained for the standard trials in the duration task and in the intensity task are superimposed on Figure 6; the resulting seven source waveforms obtained in the duration task for the five sets of trials (i.e., one per duration level) are superimposed on Figure 7.

A detailed examination of Figure 6 shows that the time course of four dipoles—the two fusiform gyri, the left frontal, and the right parietal—were similar in the two tasks for the whole time window. The two fusiform gyri displayed four peaks of activation: at 125 ms, 180 ms, 250 ms, and 865 ms following stimulus onset. We propose that this pair of dipoles would be the most important generators of the N1 components evoked at onset and offset of the visual stimulus. Indeed, the peak observed at 180 ms presumably reflects the N1 component, obtained at 170–180 ms following stimulus onset in both tasks and found to be maximal on P5 and P6 electrodes. As the standard stimulus lasted 700 ms, the peak observed at 865 ms

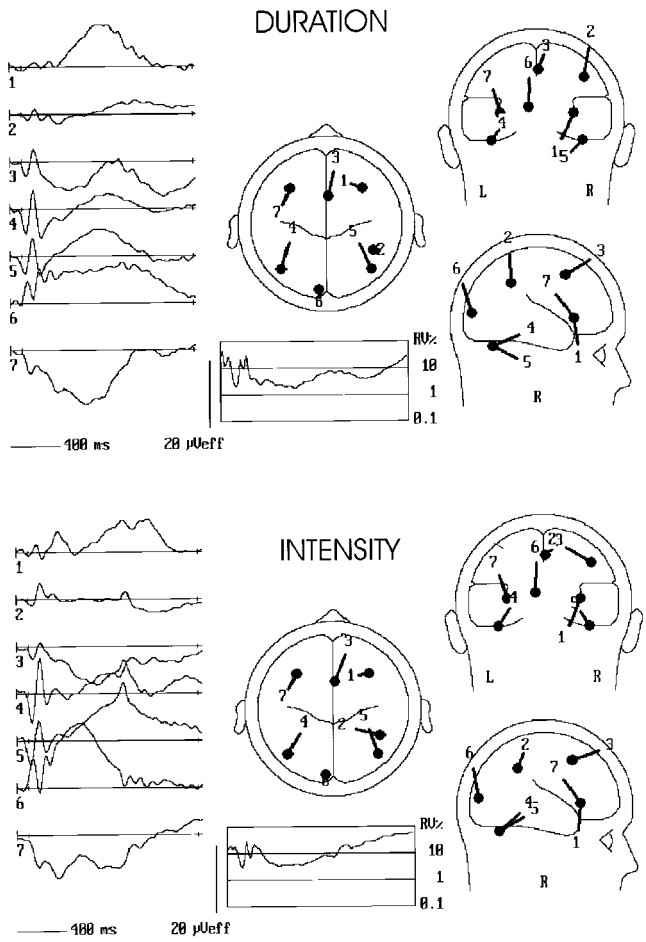

Figure 4.

Dipolar analysis for duration (top) and intensity (bottom) tasks. On the left, time course activity in the 100–1500 ms time window following stimulus onset for the seven dipoles: (1) right frontal, (2) right parietal, (3) cingulate, (4) left fusiform, (5) right fusiform, (6) cuneus, and (7) left frontal. On the right, the locations and orientations of the seven dipoles are shown on head diagrams (top, rear, and lateral views). The residual variance (RV) from 100 ms following stimulus onset up to 1500 ms following stimulus onset is diplayed in the bottom part.

would reflect the poststimulus offset N1 component. This is strengthened by the fact that the latency of this last peak covaried with the five stimulus offset times in the duration task (Fig. 7). In addition, peaks of activity in the two fusiform gyri and in the cuneus (at 125 and 250 ms following stimulus onset) would probably contribute to the P1 and P2 components of the visual event-related potential, which were maximal on POZ (see Fig. 2).

In both tasks, the left frontal dipole yielded activity from 100 ms up to 1000 ms, its amplitude was maximal during the CNV (duration task) or during the P3b (intensity task). The magnitude of the right parietal dipole seems quite flat in both tasks, only two small peaks can be distinguished at around 180 ms following stimulus onset and offset for both tasks.

For the three other dipoles—right frontal, cingulate, and cuneus—pronounced differences emerged between the two tasks. First, in the duration task, the right frontal dipole yielded largest activity between 450 and 950 ms, during the CNV. Indeed, the activity of this dipole displayed in Figure 7 parallels the ERP waveform on FCZ depicted in Figure 3; moreover, the activity of the dipole ends when the CNV resolves. By contrast, in the intensity task, the right frontal dipole only shows a low level of activity during the CNV time range. Second, in the intensity task, the magnitude waveform of the cingulate dipole parallelled the one of the left frontal dipole, whereas in the duration task, this dipole has two periods of activity. The first period between 350 and 650 ms following stimulus onset (from the beginning of the CNV development up to its maximum) and the second between 1050 and 1450 ms following stimulus onset (during the late positive component). Finally, in both tasks, the cuneus showed two peaks of activity at 125 and 250 ms following stimulus onset. These peaks of activity probably contribute to middle latency positive components of the visual ERP. From 300 ms upward, the activity of this dipole is different for each task. Whereas in the intensity task, the activity is maximal at the time of the P3b peak and diminishes when this component resolves, a sustained activity is observed all over the window in the duration task.

DISCUSSION

In this study, we mainly question the specificity of the spatio-temporal organization of cerebral areas involved when time is processed by combining ERP data with PET data previously obtained in a similar experiment. At first glance, our ERP findings replicate our PET findings: in the PET study, no significant differences between the networks activated in the two tasks were observed. In the EEG study, when the same "PET seeded model" is applied to the ERPs recorded in each task the proportion of accounted variance is approximately equivalent (84.9% in the duration task and 80.9% in the intensity one). Furthermore, in both tasks, the "PET seeded model" poorly accounts for the ERPs recorded on two scalp areas: the left frontal area and the median occipital area. When two dipoles located in these areas are added to the PET model, a better fit of ERP data is obtained for both tasks. It thus appears that the pattern of the cerebral regions acti-

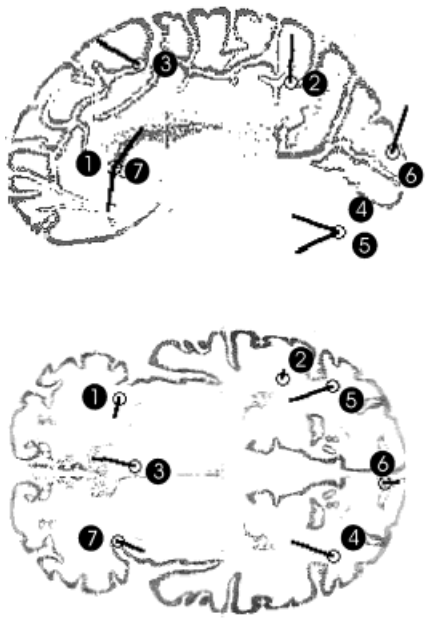

	x	y	z
1: Right Frontal	3.4	2	0.4
2: Right Parietal	4.4	-5.2	4
3: Cingulate	0.2	1	4.8
4: Left Fusiform	-4.2	-7.2	-2.4
5: Right Fusiform	4.2	-7.2	-2.4
6: Cuneus	-0.7	-9.4	1
7: Left Frontal	-3.4	2	0.4

Figure 5.
Locations of the seven dipoles in the Talairach stereotaxic coordinates.

vated during a duration discrimination task is greatly similar to that of the regions activated during an intensity discrimination task. This may seem not too surprising because activations underlie common cognitive demands in both tasks. Indeed, they both imply the same processing operations: focusing attention on the relevant feature of the stimulus, comparison with the memorized standard, and response selection as a function of a matching to sample.

However, ERP findings extend PET findings noticeably by showing that, although the network activated in the duration task is the same as the network activated in the intensity task, differences seem prominent between the time courses of the activations in the two tasks. This is particularly true for sources mainly contributing to the late latency ERP components (CNV and P3). Therefore, we will examine similarities and differences in the source waveforms in detail, particularly those relative to the extrastriate visual cortices as well as to the prefrontal and anterior cingulate areas.

No differences between tasks are observed during the first 250 ms following stimulus onset. The dipoles located in the visual associative cortices—cuneus and fusiform gyri—are the most active ones. The two fusiform gyri are the generators of the negative component that peaks at around 180 ms on parietal electrodes, and these two dipoles with the cuneus likely contribute to the occipital P1 and P2 components. The early peaks of activity of these dipoles occur exactly at the same latencies (125, 180, 250 ms, respectively) in the two tasks. This is because these dipoles generate the early ERP components evoked by the visual stimulus in both conditions. Besides, in both tasks for the standard stimulus, the last peak of activity of the fusiform gyri is observed at 865 ms; indeed, because the standard stimulus lasts 700 ms, the last peak occuring 165 ms following stimulus offset corresponds to the evoked N1 component.

According to Corbetta et al. [1991], in tasks requiring delayed response or matching to sample, that is in situations very close to the delayed "same-different" visual task we used, response selection cannot only be made on the basis of information from posterior processing areas. Memory, comparison, and decision-processing stages would involve prefontal and anterior cingulate areas that receive inputs from occipito-parietal and occipito-temporal areas. This is consistent with recent studies and clinical literature that segregate perceptual and mnemonic functions between posterior and anterior cortices, respectively [Cohen et al., 1997; Courtney et al., 1997; Goldman-Rakic, 1997]. Prefrontal and anterior cingulate areas are effectively active in our study. The differences observed in the ERP waveforms—frontal negativity in the duration task and parieto-occipital positivity in the intensity task—could undoubtely be explained by the fact that, although the sources involved are the same, their activation time courses are different.

In the intensity task, the three dipoles located in the cuneus, the anterior cingulate, and the left prefrontal area yield largest activity within the P3 interval, with the cuneus contributing maximally to the P3 component at the time of its maximum, that is, at around 520

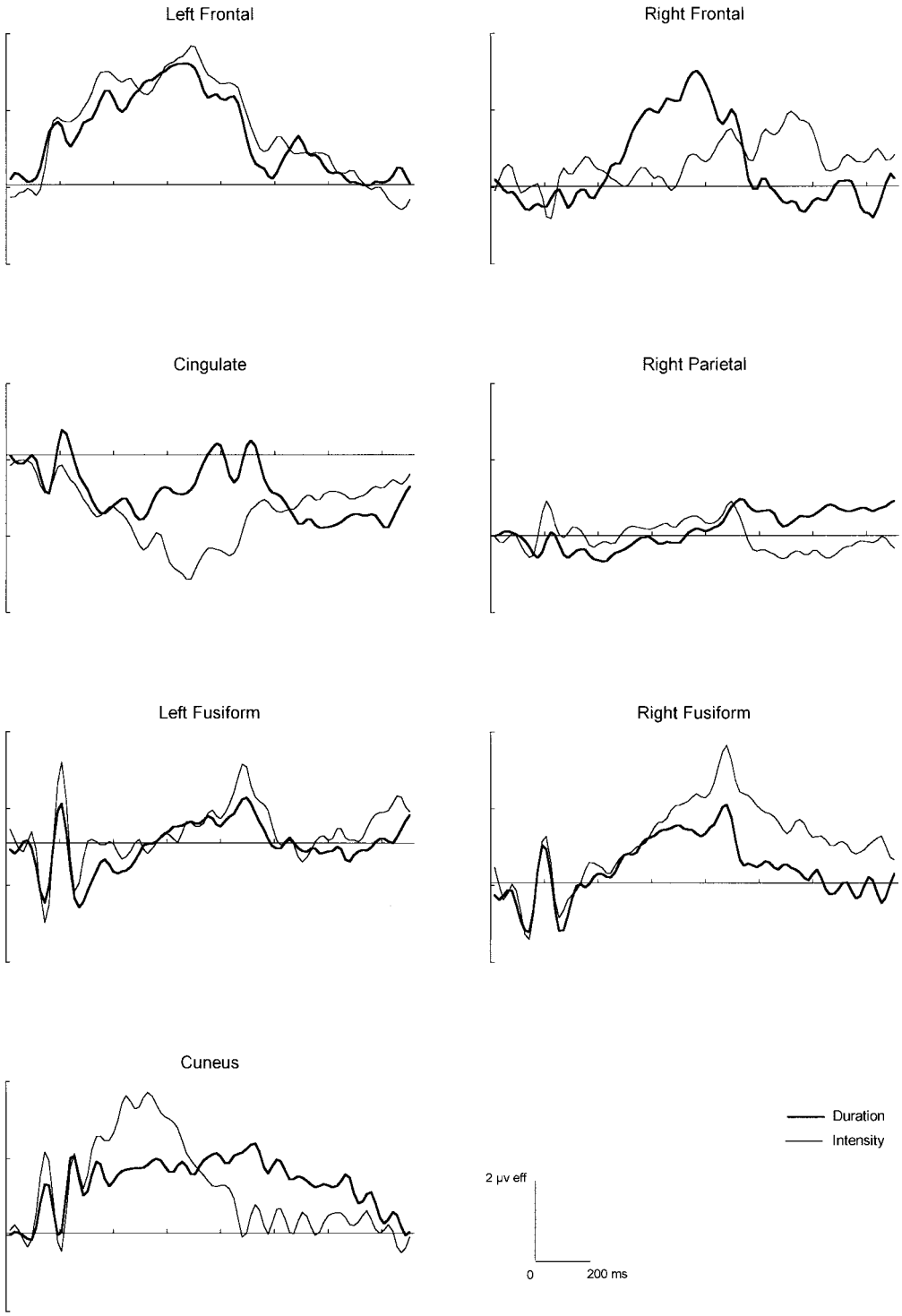

Figure 6.
Time course activity in the 100–1500 ms time window following stimulus onset for the seven dipoles for the "standard" stimulus in the duration task and the intensity task.

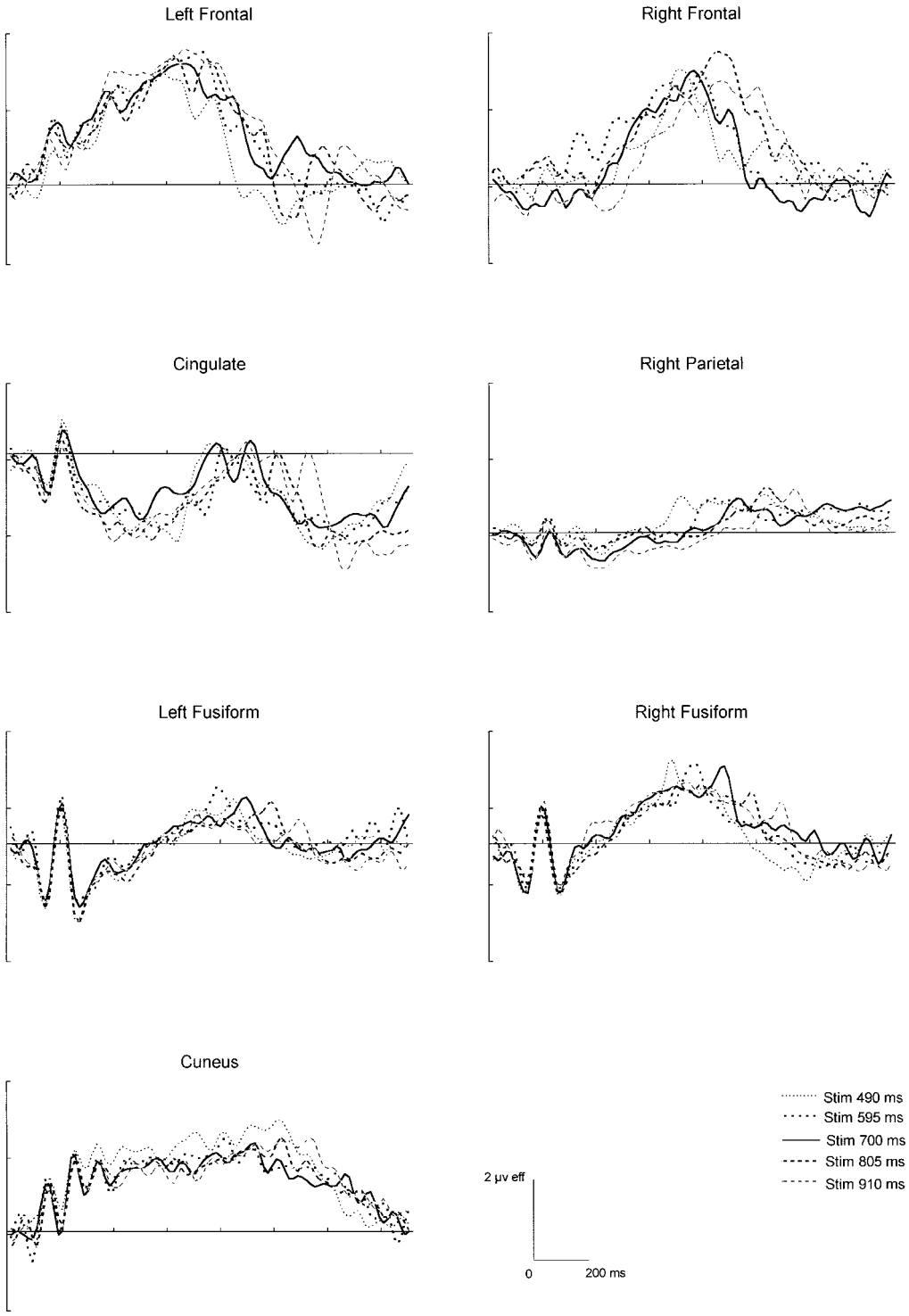

Figure 7.
Time course activity in the 100–1500 ms time window following stimulus onset for the seven dipoles in the duration task for the five stimulus durations.

ms following stimulus onset. This joint activation would underlie the comparison process, leading to the decision making, because in the intensity task, the decision can be taken during the LED illumination. Furthermore, at a latency of 600 ms, the activity of the cuneus considerably diminishes; there is no more need to further maintain sensory information on line.

In the duration task, the timing of activation of the right frontal, cingulate, and cuneus areas amply differs from that observed in the intensity task. Importantly, the right frontal area is the most active over the latency range 400–1000 ms (i.e., during the CNV). Moreover, although the CNV begins earlier (at 300 ms), the magnitude waveform of the right prefrontal dipole is very similar to the CNV waveform. Thus, the timing of its activity seems related to the duration of the LED illumination, as is the timing of the CNV (see Figs. 3 and 7). This suggests that the right frontal area has an essential role in making a decision about the duration. We assume that this role is specific to the temporal dimension of the stimulus because the right frontal area was little active in the intensity task and only following LED switch off.

In the duration task, the cuneus displays a sustained activity up to around 1300 ms following stimulus onset, that is, 600 ms on average following stimulus offset, whereas in the intensity task, the cuneus resolves at the same time as the P3 component. Furthermore, the cingulate, by contrast with the intensity task, is mainly inactive between 600 and 1000 ms in the duration task. In this task, it exhibits a period of activity between 1200 and 1400 ms following stimulus onset (see Fig. 6), likely contributing to the ERP late positive component that occurs following the CNV. The joint activity of the two dipoles—cuneus and anterior cingulate—thus subtends the end of the decision process and the response selection, which in the duration task occur late following the beginning of the trial. Indeed, the subject has to wait for the LED switch off to decide whether or not the current LED illumination duration was different from the standard, whereas in the intensity task the decision occurs almost simultaneously with the comparison process.

In sum, by evidencing differences in the time course of activations between duration and intensity processing of a visual stimulus, we are able to determine the activated areas when the subjects do really perform the duration task. Considering, first, that a joint activation of the left and right frontal areas is observed in this task only and, second, that the right frontal dipole is active during the CNV, we propose that the processing of duration information would specifically involve the right frontal area. The joint activation of the left frontal and the cuneus would be sufficient for processing intensity in a same–different task, whereas processing duration requires, in addition, the right prefrontal area. This assumption is consistent with the neuropsychological data of Harrington et al. [1998] on patients with focal left or right frontal lesions: only patients with right lesions show time perception deficit. However, more studies varying attention and memory loads are needed to validate the hypothesis of critical involvement of a right frontal area for duration information processing.

ACKNOWLEDGMENTS

The EEG research could not have been conducted without the fruitful collaboration initiated at the beginning of the PET study with P. Maquet, H. Lejeune, and F. Macar's team and their encouragement to delve further into the question we together began to study. We are grateful to our laboratory colleagues, F. Bouchet, J. C. Bourzeix, and L. Hugueville for their technical assistance, and particularly to N. Fiori, for her help in the first step of the ERPs analysis which has been presented at the 14th International Congress of EEG and Clinical Neurophysiology. We thank also the anonymous reviewers for their helpful comments on the previous version of this manuscript.

REFERENCES

Bruder GE, Towey J, Friedman D, Erhan H, Jasiukaitis P, Tenke C. 1992. Lateral asymetries of event-related potential slow waves. J Psychophysiol 6:97–110.

Cabeza R, Nyberg L. 1997. Imaging cognition: an empirical review of PET studies with normal subjects. J Cogn Neurosci 9:1–26.

Casini L, Ivry RB. 1999. Effects of divided attention on temporal processing in patients with lesions of the cerebellum or frontal lobe. Neuropsychology 13:10–21.

Casini L, Macar F. 1996. Prefrontal slow potentials in temporal compared to nontemporal tasks. J Psychophysiol 10:225–264.

Church RM. 1984. Properties of the internal clock. Ann NY Acad Sci 566–582.

Church RM, Broadbent HA. 1990. Alternative representations of time, number, and rate. Cognition 37:55–81.

Cohen JD, Perlstein WM, Braver TS, Nystrom LE, Noll DC, Jonides J, Smith EE. 1997. Temporal dynamics of brain activation during a working memory task. Nature 386:604–607.

Corbetta M, Miezin FM, Dobmeyer S, Shulman GL, Petersen SE. 1991. Selective and divided attention during visual discriminations of shape, color, and speed: functional anatomy by positron emission tomography. J Neurosci 11:2383–2402.

Coull JT, Nobre AC. 1998. Where and when to pay attention: The neural systems for directing attention to spatial locations and to time intervals as revealed by both PET and fMRI. J Neurosci 18:7426–7435.

Courtney SM, Ungerleider LG, Kell K, Haxby JV. 1997. Transient and sustained activity in a distributed neural system for human working memory. Nature 386:608–611.

Elbert T, Ulrich R, Rockstroh B, Lutzenberger W. 1991. The processing of temporal intervals reflected by CNV-like brain potentials. Psychophysiology 28:648–655.

Gibson JJ. 1975. Events are perceivable but time is not. In: Fraser JT, Laurence N, editors. The study of time, II. Berlin: Springer.

Goldman-Rakic P. 1997. Space and time in the mental universe. Nature 186:559–560.

Gratton G, Coles MGH, Donchin E. 1983. A new method of off-line removal of ocular artefacts. Electroencephalogr Clin Neurophysiol 55:468–484.

Harrington DL, Haaland KY, Knight RT. 1998. Cortical networks underlying mechanisms of time perception. J Neurosci 18:1085–1095.

Heinze HJ, Mangun GR, Burchert W, Hinrichs H, Scholz M, Münte TF, Gös A, Scherg M, Johannes S, Hundeshagen H, et al. 1994. Combined spatial and temporal imaging of brain activity during visual selective attention in humans. Nature 372:543–546.

Hinton SC, Meck WH, MacFall JR. 1996. Peak-interval timing in humans activates fronto-striatal loops. NeuroImage 3:224.

Ivry R, Keele SW. 1989. Timing functions of the cerebellum. J Cogn Neurosci 1:136–152.

Ivry R, Keele SW, Diener H. 1988. Differential contributions of the lateral and medial cerebellum to timing and to motor execution. Exp Brain Res 73:167–180.

Jonides J, Smith EE, Koeppe RA, Awh E, Minoshima S, Mintun MA. 1993. Spatial working memory in humans as revealed by PET. Nature 363:623–625.

Jueptner M, Rijntjes M, Weiller C, Faiss JH, Timmann D, Mueller SP, Diener HC. 1995. Localization of cerebellar timing process using PET. Neurology 45:1540–1545.

Lejeune H, Maquet P, Bonnet M, Casini L, Ferrara A, Macar F, Pouthas V, Timsit-Berthier M, Vidal F. 1997. The basic pattern of activation in motor and sensory temporal tasks: positron emission tomography data. Neurosci Lett 235:21–24.

Macar F, Vitton N. 1980. CNV and reaction time task in man: effects of inter-stimulus interval contingencies. Neuropsychologia 18: 585–590.

Malapani C, Rakitin BC, Levy R, Meck WH, Deweer B, Dubois B, Gibbon J. 1998. Coupled temporal memories in Parkinson's disease: a dopamine-related dysfunction. J Cogn Neurosci 10:316–331.

Mangun GR, Hopfinger JB, Kussmaul CL, Fletcher EM, Heinze HJ. 1997. Covariations in ERP and PET measures of spatial selective attention in human extrastriate visual cortex. Hum Brain Mapp 5:273–279.

Maquet P, Lejeune H, Pouthas V, Bonnet M, Casini L, Macar F, Timsit-Berthier M, Vidal F, Ferrara A, Degueldre C, et al. 1996. Brain activation induced by estimation of duration: a PET study. Neuroimage 3:119–126.

Michon JA. 1967. Timing in temporal tracking. Assen, The Netherlands: Van Gorcum.

Michon JA. 1990. Implicit and explicit representations of time. In: Block RA, editor. Cognitive models of psychological time. Hillsdale, NJ: Lawrence Erlbaum Associates. p. 37–58.

Pardo JV, Fox PT, Raichle ME. 1991. Localization of a human system for sustained attention by positron emission tomography. Nature 349:61–64.

Rao SM, Harrington DL, Haaland KY, Bobholz JA, Cox RW, Binder JR. 1997. Distributed neural systems underlying the timing of movements. J Neurosci 17:5528–5535.

Ruchkin DS, McCalley MG, Glaser EM. 1977. Event related potentials and time estimation. Psychophysiology 14:451–455.

Scherg M. 1992. Functional imaging and localization of electromagnetic brain activity. Brain Topogr 5:103–111.

Treisman M, Brogan D. 1992. Time perception and the internal clock: effects of visual flicker on the temporal oscillator. Eur J Cogn Psychol 4:41–70.

Walter WG, Cooper R, Aldridge VJ, McCallum WC, Winter AL. 1964. Contingent negative variation: an electric sign of sensorimotor association and expectancy in the human brain. Nature 203:380–384.

Woldorff MG, Fox PT, Matzke M, Lancaster JL, Veeraswamy S, Zamarripa F, Seabolt M, Glass T, Gao JH, Martin CC, et al. 1997. Retinotopic organization of early visual spatial attention effects as revealed by PET and ERPs. Hum Brain Mapp 5:280–286.